Polymer Interdiffusion near an Attractive Solid Substrate

Eric K. Lin,* Wen-li Wu, and Sushil K. Satija†

Polymers Division and Reactor Radiation Division, National Institute of Standards and Technology, Gaithersburg, Maryland 20899

Received April 1, 1997; Revised Manuscript Received August 9, 1997[⊗]

ABSTRACT: Neutron reflectometry is used to study interdiffusion in bilayers of hydrogenated and deuterated poly(methyl methacrylate) (PMMA) on silicon substrates where the polymer−substrate interaction energy is strongly attractive. The effect of the polymer−substrate interaction energy on the interdiffusion rate as a function of distance from the surface is investigated. Samples are prepared with lower layer thicknesses of the deuterated PMMA ranging from 35 to 335 Å or 0.4 to 3.6 radii of gyration (R_g) of the bulk polymer chain. The rate of interdiffusion is found to be strongly dependent upon the lower film size. Polymers in films less than R_g in thickness have effective diffusion constants 2 orders of magnitude smaller than polymers in the thickest films. The effective range of the substrate on the interdiffusion dynamics is found to be between 300 and 400 Å or 3 R_g and 4 R_g. The observed dynamics are attributed to the different polymer chain conformations at varying distances from the solid surface.

1. Introduction

The properties of polymer chains near an impenetrable surface have received much recent attention and are important in applications such as electronics packaging, composite materials, coatings, and adhesion.[1] Oftentimes, the performance of the materials and devices is dependent upon knowledge about the structure and dynamics of the interfacial polymer. Knowledge of the bulk polymer properties is not useful in these areas because the equilibrium structure and dynamics of the interfacial polymer chains are quite different from those of the bulk polymer. Geometric constraints from the surface alter the conformation of the polymer chains, and the interaction energy between the polymer and the surface can provide additional enthalpic contributions to the interfacial polymer properties.

Several recent experiments have shown that both chain confinement and the interaction of the polymer with the substrate strongly affect the properties of interfacial polymers. Orts et al.[2] and Keddie et al.[3] observed that ultrathin polystyrene films on silicon oxide surfaces (with a weakly attractive interaction energy) exhibit a lower glass transition temperature, T_g, than the bulk polymer. Additionally, Reiter[4] observed that polystyrene films dewetted silicon oxide surfaces at temperatures below the bulk polymer T_g, providing evidence of enhanced chain mobility. However, for ultrathin polymer films with strongly attractive interactions between the polymer and the substrate, the T_g increased by as much as 30 °C and the thermal expansion coefficients decreased relative to those of the bulk polymer.[5−7] From these studies, it was estimated that the influence of the substrate reached several hundred ångstroms, or several times the length scale of the unperturbed polymer chain.[5] The changing thermal properties observed in these experiments reflect differences in the polymer chain dynamics. Increases in T_g imply that the polymer dynamics have slowed down near an attractive interface, and decreases in T_g suggest that the polymer chains have greater mobility than in the bulk polymer. Recent measurements of T_g in freely standing thin polystyrene films show large decreases in the observed T_g, demonstrating the large effects the free surface and the substrate have on the polymer properties.[8]

In many applications, information about the properties of interfacial polymers in contact with the bulk polymer are needed. Only limited experimental information about these interfacial polymer properties is available because of the challenge of probing buried interfaces and distinguishing the interfacial polymer from the bulk polymer. Progress has been made by several groups using techniques such as dynamic secondary ion mass spectrometry (SIMS) and neutron reflectometry to study buried interfaces with deuterated components; providing a convenient way to selectively label the interfacial polymer. Zheng et al.[9] used SIMS and van Alsten et al.[10] used neutron reflectometry to study the bulk rate of diffusion from a solid surface of polystyrene on different substrates and of poly(methyl methacrylate) on a silicon substrate, respectively. In both studies, decreases in the effective diffusion constants or chain mobilities for polymer chains near the surface are observed. It was suggested that the decreased chain mobility arises from an increased friction factor due to the attractive interaction energy between the polymer segments and the substrate.[9] This argument suggests that at distances greater than $\approx R_g$ from the surface, the polymer dynamics should resemble bulk behavior. Computer simulations studying the center of mass diffusion of oligomer chains near surfaces have also shown that the diffusion of chains from the surface decreases relative to bulk values with an effective range of influence of about R_g. Interestingly, the diffusion parallel to a neutral surface was enhanced because the chains are oriented parallel to the surface.[11−14] Longer ranged perturbations from bulk chain behavior were observed for supercooled melts between neutral walls.[14,15] No computer simulations to date have been able to examine polymer chain melt dynamics above the entanglement molecular weight.

In this work, we are interested in measuring chain mobility in polymeric thin films. We use neutron reflectometry to measure the movement of polymer chains near an attractive substrate from bilayer interdiffusion experiments. Information about the polymer chain mobility can be obtained from the measurement of the rate of interdiffusion between polymer layers. For

* To whom correspondence should be addressed at the Polymers Division.
† Reactor Radiation Division.
⊗ Abstract published in *Advance ACS Abstracts,* October 15, 1997.

S0024-9297(97)00442-7 CCC: $14.00

Table 1. Physical Characteristics of the Polymers Used in This Study

polymer	mol wt	M_w/M_n	R_g (Å)[36]
hPMMA	143 000	1.04	99
dPMMA	135 000	1.10	93

bulk systems, where the interface is far from the substrate surface, much has been learned about the interdiffusion. The initial stages of bulk polymer interdiffusion using bilayers of polystyrene were studied using neutron reflectometry by Stamm et al.[16] and Karim et al.[17,18] Bulk interdiffusion for poly(methyl methacrylate) (PMMA) bilayers was recently measured using neutron reflectometry by Kunz and Stamm.[19] In these studies, the data are found to be consistent with features from the reptation model for polymer dynamics,[20,21] describing the polymer chain mobility along its contour path through a "tube" defined by the matrix of surrounding chains. Additional interdiffusion experiments using specially labeled triblock copolymers have also provided enhanced evidence validating the reptation model in comparison with other dynamical models.[22]

In this study, we use bilayers of poly(methyl methacrylate) (PMMA) near the native oxide surface of silicon; a system with a strongly attractive interaction energy between the polymer segment and the substrate. We prepare samples with different lower layer thicknesses and monitor the interfacial profile as a function of the annealing time. Varying the lower layer thickness results in changing the polymer conformations by confining the polymer in films smaller than $2R_g$. Not only will the attractive interaction between the surface and the polymer slow the polymer dynamics, but also additional effects from the confined chain conformations may appear. The interdiffusion results also provide information about the chain dynamics at the free surface of thin polymer films. A series of samples provides an important estimate of the length scale at which the substrate no longer influences the chain dynamics at the polymer−polymer interface.

2. Experimental Section

2.1. Sample Preparation. The hydrogenated poly(methyl methacrylate) with a molecular weight[23] of 143 000 and a polydispersity index of 1.04 was purchased from Polymer Laboratories.[24] The deuterated PMMA was synthesized using a group-transfer polymerization method and has a molecular weight of 135 000 and a polydispersity index of 1.10. Both polymers are approximately 57% syndiotactic, 37% atactic, and 6% isotactic. The polymer characteristics are summarized in Table 1.

The bilayers were prepared on polished silicon wafers 75 mm in diameter and 5 mm thick. After the native oxide layer was stripped from clean wafers in a buffered etch solution, the wafer surface was placed in a UV/ozone cleaner for 3 min, forming an oxide surface 15−25 Å thick. Thin layers of varying thicknesses of the deuterated polymer were prepared by spin coating at 2000 rpm solutions of the polymer in o-xylene, mass fractions 0.3−2.0%. The deuterated layers were annealed under vacuum at 150 °C for at least 6 h above the glass transition of the polymer (T_g = 115 °C, as determined from DSC measurements) and very slowly cooled to room temperature. The sample thicknesses and polymer/interface roughnesses were then characterized from the X-ray reflectivity. For each sample, the measured roughnesses for the substrate/polymer interface and the polymer/air interface were less than 10 Å.

The overlayers were prepared using the floating technique. Thin polymer layers were prepared from solutions of the hydrogenated PMMA in *o*-xylene, mass fractions 2.0−2.75%, by spin coating onto glass slides at 2000 rpm. The sides of the slides were scored with a razor blade and the films (800−1000 Å) were floated from deionized water onto the deuterated layers. The resulting bilayers were kept under vacuum at 25 °C for at least 15 h to remove excess water. The prepared bilayer samples and their characteristics are given in Table 2.[25] The lower film thickness is normalized with R_g, the characteristic size of the polymer in the bulk.

For the interdiffusion experiment, the samples were annealed in a large aluminum block held at 150 °C within a vacuum oven and were periodically removed from the oven to measure the reflectivity. In past interdiffusion studies, the samples were annealed at different temperatures to take advantage of the time−temperature superposition of the polymer dynamics through the use of the Williams−Landel−Ferry (WLF) equation.[26] Here, only a constant temperature of 150 °C is used. Although the bulk relaxation times can be rescaled using the WLF equation, it is not clear how the time scales of the polymer dynamics are rescaled with respect to the polymer−surface interaction energy. After being annealed for a set time, the samples were rapidly quenched to room temperature on a cool aluminum block. Typically, the sample is cooled to room temperature within 30 s.

2.2. Neutron Reflectometry. The neutron reflectivity measurements were performed at the National Institute of Standards and Technology NG-7 reflectometer at the specular condition. The wavelength was 4.768 Å. The neutron beam was sent through the silicon substrate with a transmission of ≈0.90 of the beam intensity as measured through air. All reflectivity measurements were taken at room temperature. The reflectivity is measured at different incident angles and presented as a function of the scattering vector in the perpendicular direction, $Q = (4\pi/\lambda) \sin\theta$ where θ is the incident angle and λ is the wavelength of the beam.

The modeling and fitting of the reflectivity data were performed with nonlinear least-squares fits using the recursive multilayer method.[27] The physical quantity used to fit the data is the elastic coherent-scattering per unit volume, Q_c^2. Q_c^2 is related to the neutron scattering length, b, through the expression $Q_c^2 = 16\pi nb$ where n is the number density of scattering nuclei. The Q_c^2 values for bulk silicon, deuterated PMMA, and hydrogenated PMMA are 1.06×10^{-4} Å^{-2}, 3.50×10^{-4} Å^{-2}, and 5.15×10^{-5} Å^{-2}, respectively. The Q_c^2 values for the deuterated and hydrogenated components are different, leading to strong contrast between almost chemically identical species.

3. Results

In Figure 1, the neutron reflectivity data for sample E at four different annealing times are shown along with the best fit curves. The real space profiles in terms of Q_c^2 corresponding to the best fit to the reflectivity data are shown in Figure 2. In the as cast bilayer, several distinct interference fringes in the reflectivity curve are observed indicating that the interface is sharply defined. The initial thickness of the deuterated layer determines the Q spacing between the minima or maxima of the reflectivity curve. As the annealing time is increased, the interface between the layers begins to broaden and results in a gradual loss of the higher order minima in the reflectivity curves at higher Q values. Additionally, higher order oscillations become visible at later annealing times, arising from reflections from the overall thickness of the bilayer sample. The small differences between the experimental data and the fitted curves at small values of Q are due to alignment errors in the slit openings and the beam footprint. These errors are not significant at larger Q values.

Initially, we fit the reflectivity data using an error function profile between the two layers since it is the solution for normal Fickian diffusion. We find the error function provides good fits at all annealing times to the data from the samples with the thinnest deuterated

Table 2. Physical Characteristics of the Prepared Bilayer Samples[a]

sample name	thickness, h, dPMMA (Å)	h/R_g	thickness, h, hPMMA (Å)	σ (Å) hPMMA/air	σ (Å) Si/dPMMA	$D_{eff} \times 10^{-16}$ (cm^2/s)
A	35 ± 1	0.38	789 ± 1	36 ± 1	10.2 ± 0.5	$3.6 \times 10^{-4} \pm 0.3 \times 10$
B	70 ± 1	0.75	804 ± 1	15 ± 1	10.9 ± 0.5	$7.5 \times 10^{-3} \pm 0.3 \times 10^{-3}$
C	148 ± 1	1.59	842 ± 1	19 ± 1	10.0 ± 0.5	0.09 ± 0.01
D	203 ± 1	2.18	1420 ± 1	20 ± 1	10.5 ± 0.5	0.10 ± 0.01
E	334 ± 1	3.60	768 ± 1	20 ± 1	12.0 ± 0.5	0.25 ± 0.02

[a] Total thicknesses of each layer and the roughness of the hPMMA/air interface were determined from X-ray reflectivity measurements. The values of the roughness for the Si/dPMMA interface are from the best fits with the neutron reflectivity data.[25]

Table 3. Volume Fraction of Deuterated Segments at the Silicon Surface, Φ_s, and the Interfacial Width from the Best Fits to the Neutron Reflectivity Data for Different Annealing Times at 150 °C[a]

	A		B		C		D		E	
time (min)	Φ_s	$\Delta\sigma$ (Å)	Φ_s	$\Delta\sigma$ (Å)	Φ_s	$\Delta\sigma$ (Å)	Φ_s	$\Delta\sigma$ (Å)	Φ_s	$\Delta\sigma$ (Å)
0	1.00	4 ± 2.0	1.00	8 ± 1.0	1.00	5 ± 1.0	1.00	4 ± 1.0	1.00	4 ± 1.0
2	0.97	17 ± 2.0	0.99	24 ± 2.0	1.00	29 ± 2.0	1.00	23 ± 2.0	1.00	30 ± 2.0
7	0.92	18 ± 2.0	0.98	28 ± 2.0	0.99	32 ± 3.0	1.00	29 ± 3.0	1.00	35 ± 3.0
22	0.88	19 ± 2.0	0.95	31 ± 3.0	0.99	44 ± 3.0	1.00	39 ± 3.0	1.00	41 ± 3.0
42	0.86	20 ± 2.0					1.00	48 ± 7.0		
67	0.86	20 ± 2.0	0.93	37 ± 3.0			1.00	52 ± 5.0	1.00	63 ± 5.0
112	0.81	20 ± 2.0	0.90	39 ± 4.0			1.00	68 ± 5.0	1.00	93 ± 6.0
117					0.99	73 ± 6.0				
187	0.78	21 ± 2.0	0.88	42 ± 4.0			1.00	83 ± 6.0	1.00	114 ± 12.0
192					0.99	87 ± 7.0				

[a] Φ_s is determined from the Q_c^2 values at the dPMMA/Si interface.[25]

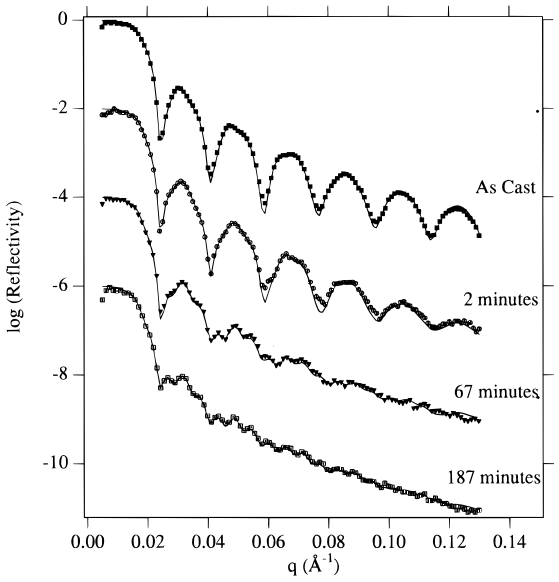

Figure 1. Typical neutron reflectivity data from sample E for four annealing times at 150 °C. The data are shown with the symbols and the best fits are given by the solid lines. The curves are offset vertically for clarity.

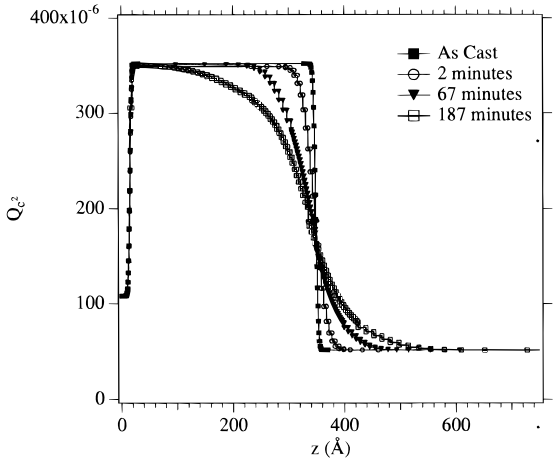

Figure 2. Real space profiles for the fits to the neutron reflectivity data from sample E for four annealing times at 150 °C. The quantity, Q_c^2, the elastic scattering length per unit volume, is plotted vs the distance from the surface. Q_c^2 is linearly related to the deuterium concentration. The curves from the as cast film and 2 min anneal utilize the error function to fit the data. The curves from the 67 and 187 min anneals are not fitted with an error function. A modified profile is used leading to a reduction by at least a factor of 2 of χ^2 (from χ^2 test) in the quality of the fit.

layers, samples A and B. For thicker lower layers, the error function profile adequately fits the data at the shorter annealing times (<22 min). However, for longer annealing times, non-error-function Q_c^2 profiles are required to fit the data. This requirement has been noted in bulk interdiffusion studies using polystyrene[16,18] and PMMA.[19] The need for a different functional fit is consistent with the reptation description of polymer dynamics for diffusion distances less than R_g.[28] The real space profile generally has a steep central part corresponding to the initially sharp interface with broader concentration gradients on either side of the interface corresponding to movement by the chain ends. The modified profiles used here to fit the data have the same characteristic shape and are generated using four separate layers with different error function profiles between them with varying characteristic widths. Figure 3 shows the difference between an error function fit and the modified model fit at an intermediate annealing time for sample C. The detailed profile fit to the data generally decreases the χ^2 (from a χ^2 statistical test) value of the fit by at least a factor of 2. As an additional constraint, we check to ensure that mass is conserved with the modified real space profiles. The subtle differences between the two real space profiles demonstrates the sensitivity of the reflectivity technique to the functional form of the Q_c^2 profile.

The primary parameter extracted from the fits to the reflectivity data is the interfacial width, σ. To characterize the size of the interfacial width, the second moment of the derivative of the real space profile is

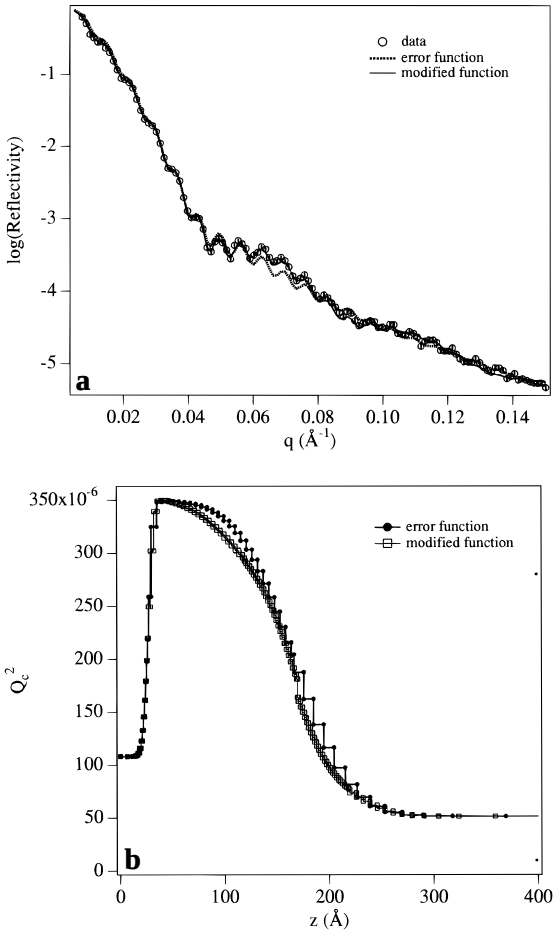

Figure 3. (a) Neutron reflectivity data from sample C after 117 min at 150 °C given by the symbols. The best fit curve using an error function profile is given by the dotted line and the best fit with a more detailed profile is given by the solid line. (b) Real space profiles in terms of the elastic scattering length, Q_c^2, for the error function and the more detailed profile.

used. For an error function, σ is the variance of the derivative of the real space profile. The initial roughness at the interface from the sample preparation is quadratically subtracted from the measured interfacial width through $\Delta\sigma = (\sigma^2 - \sigma_0^2)^{1/2}$, where σ_0 is initial roughness of the interface. The results of the fits including the volume fraction of deuterated polymer at the silicon surface, Φ_S, and $\Delta\sigma$ are summarized for all the samples and annealing times in Table 2. The reported values for $\Delta\sigma$ at 0 min are the values for σ_0. The volume fraction of the deuterated component at the substrate surface is determined from the Q_c^2 values at the dPMMA/silicon interface and provides a measure of the rate of exchange between deuterated and hydrogenated segments at the substrate surface.

In Figure 4, the interfacial width of each sample as a function of time for each sample is plotted using logarithmic scales. The data from interdiffusion experiments by Kunz and Stamm[19] for a different molecular weight PMMA bilayer system (M_w = 85 500) representing the change in the interfacial width free from the effects of the underlying substrate are also shown. Their data are rescaled for molecular weight from scaling arguments[20,21] and for temperature through the WLF equation. Within the reptation framework, the bulk bilayer interdiffusion rate is expected to have varying power law exponents for the time dependence of $\Delta\sigma$ for short time interdiffusion ($\Delta\sigma < R_g$). Three characteristic time scales are defined:[20,21] the entanglement relaxation time, τ_e, corresponding to the time scale for the Rouse relaxation of the chain within the reptation tube, the reptation time, τ_R, corresponding to the chain relaxation time constrained by the tube, and τ_D, representing the time after which the chain has disengaged from the tube and normal Fickian diffusion is recovered. The power law dependences for $\Delta\sigma$ between characteristic times have been determined by Doi and Edwards.[21] For $\tau_e < t < \tau_R$, $t^{1/8}$ is expected, for $\tau_R < t < \tau_D$, a $t^{1/4}$ dependence is predicted, and finally, for $t > \tau_D$, $t^{1/2}$ is expected. For PMMA and the annealing temperature of these experiments, we use the values reported by Kunz and Stamm[19] and estimate that for this system, τ_e = 0.072 min, τ_R = 0.26 min, and τ_D = 8.53 min.

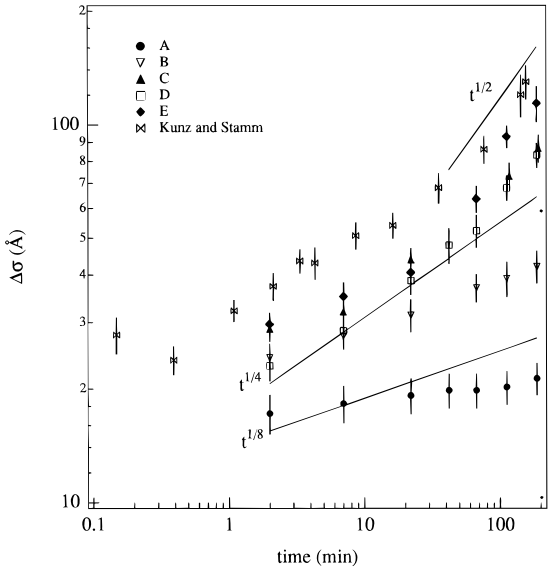

Figure 4. The interfacial width, $\Delta\sigma$, plotted using logarithmic scales as a function of the annealing time at 150 °C for bilayer samples with different lower layer thicknesses.

Initially prepared films have very sharp interfaces between the dPMMA and the hPMMA layers with $\Delta\sigma$ between 5 and 8 Å. At the shortest annealing times (2 min), a rapid broadening of the interface is observed of approximately 20−30 Å for each sample. This initial broadening has been observed in previous experiments[16,17,19] and has been attributed to the fast Rouse relaxation modes within the reptation tube and/or to capillary wave effects. This initial broadening is observed even in sample B with a lower layer 70 Å thick, indicating that the very fast initial broadening is not dependent on the lower film thickness until the film becomes as thin as the length scale of this fast diffusion process. The slightly smaller amount of initial broadening in sample A is not surprising since the initial layer size is comparable to that of the expected tube diameter, 25 Å.[19]

The change in time dependent scaling of $\Delta\sigma$ is evident for the samples with thicker lower layer thicknesses (C, D, and E). The samples with thinner lower layers (A and B) do not exhibit the same qualitative changes in the time dependent scaling. The experimental points for each system are all at times greater than τ_e and τ_R. The slow $t^{1/8}$ behavior would not be expected to be apparent within these experiments for bulk bilayer samples because of the short time scales for τ_e and τ_R relative to the experimental time. However, for sample B, $t^{1/8}$ scaling is present over the entire annealing cycle suggesting that the movement of the polymer chains

near the interface remains restricted. Sample A exhibits an even slower scaling behavior not previously observed. Instead of the chain dynamics confined to a reptation tube, the slow dynamics arise from the polymer chains being pinned to the silicon surface and from effects from the structure of the polymer chains near the surface.

The deuterated volume fraction at the surface for samples A and B does not rapidly decrease with time indicating that the hydrogenated chains do not readily replace the deuterated segments. Similar behavior was observed in the work of van Alsten et al.[10] where they follow the bulk chain displacement near an interface. They do not observe any bulk replacement of the deuterated layer near the surface until temperatures 50 °C above the glass transition of the polymer,[10] but they are not able to resolve the details of the penetration of the ultrathin film into the overlayer. In our experiments, the surface concentration of the initial polymer segments also does not significantly change even after several hours of annealing, but we observe a slow broadening of the interface, indicating that the polymer segments do diffuse into the overlayer with motion constrained by the interaction energy between the substrate and the polymer segments. This behavior is similar to the long timescales observed[29] and predicted[30] for the mixing dynamics between end-grafted polymer chains and a homopolymer matrix. An additional effect which may play a role in the segment displacement near a substrate is the difference in the interaction energy between the deuterated and hydrogenated polymer segments with the surface. It has been observed in polystyrene systems that the deuterated polymer preferentially segregates to the silicon surface.[31] The quantitative effect of this difference on PMMA polymer dynamics is not well-established at this time.

Samples C, D, and E most closely follow the $t^{1/4}$ scaling over the time scale of the experiments. This scaling behavior is consistent with earlier interdiffusion studies interpreted within the reptation framework.[17] However, the relative values of $\Delta\sigma$ differ at the same annealing times suggesting that additional effects may perturb the interdiffusion dynamics. None of the data sets clearly reaches the Fickian diffusion limit with a $t^{1/2}$ dependence. In general, it is difficult to observe the time dependent behavior of the deuterated segment concentration at the Fickian diffusion limit because the neutron reflectometry technique is not as sensitive to interfacial widths greater than ~150 Å.

From Figure 4, the values for $\Delta\sigma$ at the longest annealing times are dependent upon the initial film thickness. At the longest annealing times, the value of $\Delta\sigma$ for the smallest lower layer is an order of magnitude smaller than that of the thickest layer. Even though similar changes in the scaling behavior are observed for samples with $h/R_g > 1.5$, the observed interdiffusion rate varies with the initial lower layer thickness. To roughly characterize the interdiffusion rate, we linearly fit the data from a plot of $\Delta\sigma$ as a function of $t^{1/2}$ for each sample in Figure 5 over the time scale of the experiments. If the diffusion process were purely Fickian, then the data would be linear in this type of plot and the slope of the resulting line would be proportional to the bulk diffusion constant. The scaling behavior in Figure 4 indicates that the Fickian diffusion limit is not definitively reached in these experiments. Additionally, the intercepts from the fits are not zero because of the rapid initial broadening at very short times which is

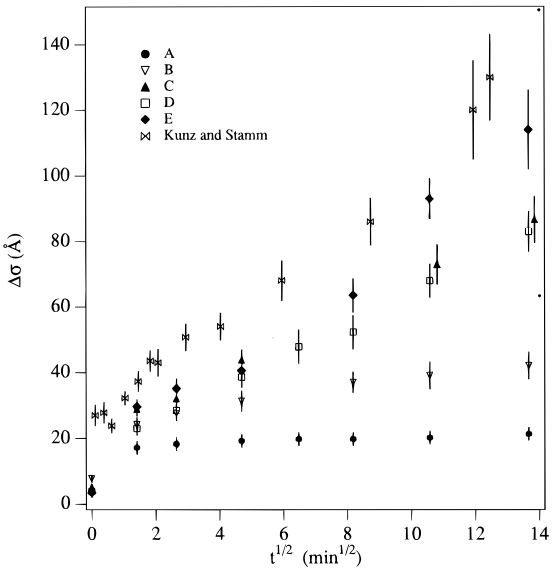

Figure 5. Interfacial width, $\Delta\sigma$, plotted as a function of the square root of the annealing time at 150 °C for bilayer samples with different lower layer thicknesses. At time zero, $\Delta\sigma$, is the as prepared interfacial roughness, σ_0.

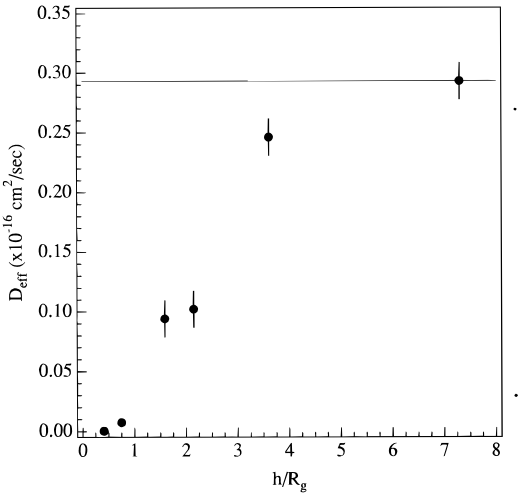

Figure 6. Effective diffusion coefficient, D_{eff}, determined as described in the text as a function of the lower layer thickness normalized on the radius of gyration, R_g, of the polymer. D_{eff} is not strictly the mutual or tracer diffusion constant of the polymer chain but is a parameter characterizing the rate of interdiffusion near an attractive surface.

not present in Fickian diffusion. The diffusion constant determined from the fits is not the bulk diffusion constant, but is interpreted as an effective segment diffusion constant, D_{eff}, providing a measure of the interdiffusion rate including the different processes described earlier in the reptation framework. We have also used the value of $\Delta\sigma$ at the longest annealing times to determine an effective diffusion constant with similar results.

From the variation of D_{eff} with the initial lower film size, we can estimate the length scale at which the substrate continues to perturb the rate of interdiffusion. The effective diffusion constants for each sample are given in Table 2 and shown in Figure 6 as a function of the initial layer thickness normalized on R_g. Even the values for D_{eff} for the thickest samples are expected to be lower than those determined using longer length scale techniques such as SIMS because they are more heavily weighted by the slower diffusion rates at the short times studied here. For comparison, the bulk

diffusion constant for the molecular weight PMMA used here at 150 °C from gold marker experiments of Liu et al.[32] was determined to be 0.88×10^{-16} cm^2/sec after rescaling for molecular weight and temperature. For our thickest sample and the Kunz and Stamm[19] data, D_{eff} is found to be 0.25×10^{-16} cm^2/s and 0.29×10^{-16} cm^2/s, respectively, in reasonable agreement with the results from the gold marker experiments.

The effective diffusion constant is less than the "bulk" value for films up to 3 R_g thick. We find that the effective diffusion constants for the thinnest layers are nearly 2 orders of magnitude smaller than the bulk values. Zheng et al.[9] observed a similar significant decrease in the effective diffusion constant for 50 Å thick layers of polystyrene on a silicon substrate even though the interaction energy between polystyrene and silicon oxide is less than that of PMMA and silicon oxide. Both experiments study initial films less than or approximately 1 R_g in thickness. Within these films, the polymer chains are severely distorted and are in intimate contact with the substrate. Once long chains have many contacts with the surface, even a small interaction energy may effectively fix a polymer chain. Zheng et al.[9] determine a single effective diffusion constant because of the depth resolution of SIMS to ~90 Å. Our experiments show that the diffusion rate is dependent upon the film size. Significant differences in the effective diffusion constant are observed between films 0.5−2 R_g, both within the criteria used by Zheng et al.[9] The initial state of the polymer chains plays an important role in the dynamics and the experimental data suggests the diffusion rate is dependent upon distance from the substrate and the characteristic size of the adsorbed chain structure.

From Figure 6, we estimate the effective range of the substrate on the the dynamics of the polymers to be between 3 and 4 R_g, ≈300 Å in this system. This length scale is consistent with that extracted from thermal expansion experiments of polymer thin films on an attractive surface[5,7] and the length scale in computer simulations at which all polymer chains are expected to have distorted conformations (≈2 R_g because of the initial presence of two confining interfaces).[11,15] Interestingly, the 3−4 R_g length scale for which a change in D_{eff} from bulk properties is observed is similar to the value determined by Forrest et al.[8] for the observed T_g suppression of freely suspended polystyrene films suggesting that changes from "bulk" properties are related to distorted chain conformations. However, this length scale is much less than that reported by Frank et al.[33] for the lateral diffusion constant of polystyrene chains. They find that the bulk diffusion constant is reduced for films up to 25 times the polymer R_g and is proportional to the length of the fully extended chain.

4. Discussion

The rate of interdiffusion for polymer bilayers near an attractive surface is dependent upon both the interaction energy of the polymer segment with the substrate and the conformations of the chains. Experimental observations can be qualitatively explained by considering distorted chain conformations and the substrate interaction energy. Initial chain conformation determines the distribution of the chain ends in the film, number of contacts a chain has with the surface, and changes in the local environment of each chain due to the anisotropic confinement of the polymer. Interaction energy with the substrate provides an energetic factor hindering the removal of a chain from the surface. The effects of these two factors on the initial stages of polymer interdiffusion rate are interdependent. An attractive substrate interaction energy with each polymer segment locally slows the polymer chain dynamics, but the large scale motion is dependent upon the number of segments per chain in contact with the surface as well as the local structure of the surrounding polymer chains. Interpretation of the experimental results is strongly dependent upon the lower film size because each sample represents the dynamics of polymer chains in different configurations. The observed differences in the rate of interdiffusion show the importance of the initial film size layer in interpreting other experimental data.[9]

Within the reptation picture, where polymer chain movement occurs through the chain ends, an important parameter is the number of chain ends located at the polymer−polymer interface. As a limiting case, we assume all chain ends within R_g of the interface are located at the interface. The areal density of chain ends at the interface given a lower film thickness, d, can be estimated to be

$$\rho_e = \frac{2d\rho}{N}, \qquad d \le R_g \tag{1}$$

where ρ is the monomer density and N is the degree of polymerization. The maximum value of ρ_e is attained for the largest bilayers since only chains within R_g of the interface are presumed to have chain ends at the interface. As the lower film thickness decreases below R_g, the density of chain ends at the interface decreases. Additionally, the chain end density will not be equal on both sides of the interface because of the difference in the prepared films. The effects of the density of chain ends is weak as eq 1 is linearly dependent on the film thickness and we observe decreases in D_{eff} in Figure 6 larger than can be attributed solely to a decrease in ρ_e. The experimental data can be interpreted by considering three film size regimes with dynamics reflecting the environment of the chains at the polymer−polymer interface.

For samples with lower layers that are less than R_g thick, highly distorted chain conformations are expected and the interdiffusion experiments here become similar to experiments involving polymer desorption in solution[34] and tethered polymer chains diffusing into a homopolymer matrix.[29] Within these samples, the backbone of the polymer chains is primarily oriented parallel to the substrate surface. Not only is ρ_e lower for these films, the flattened polymer chains have many more contacts with the substrate than polymers in the thicker bilayer structures. Nearly all of the labeled polymer chains in samples A and B are expected to have segments in contact with the substrate. The result is that the energy needed to remove an entire chain so that it may freely diffuse into the bulk domain is very large. The Boltzmann factor for the removal of the chain is on the order of

$$\tau \approx \exp(-N_c E_a / kT) \tag{2}$$

where N_c is the number of monomer contacts with the surface, E_a is the substrate−polymer segment interaction energy, k is Boltzmann's constant, and T is the absolute temperature. Since N_c is large, the Boltzmann factor is very small, and it is unlikely that the entire chain is removed over the experimental time scale. The

magnitude of the interaction energy, E_a, may not be too important for polymers with large N_c since τ will still be very small and differences on the laboratory time scale may not be visible. The dynamics in these films appear to be dominated by the rate of the segment−segment exchange rate governed by E_a.

When the lower layer thickness is between R_g and 2 R_g, some chain distortion is still expected throughout the film. There is some reduction in the number of chain ends at the interface and the number of contacts for chains at the polymer−polymer interface contacting the substrate is smaller than for samples less than R_g thick. In this thickness range, the decrease in the rate of interdiffusion is most likely related to the adsorbed layer structure of the polymer chains closest to the substrate. The presence of loops and trains in the adsorbed polymer structure may resemble a fixed network reducing the rate of interdiffusion. As the overlayer chains move toward the substrate, the increasing structure of the polymer layers close to the substrate as well as the slower dynamics of the adsorbed chains hinders the interdiffusion rate. Chains close to the substrate surface are less likely to move from the substrate for similar reasons given for the thinnest layers. The clear reduction in the interdiffusion rate for these film sizes demonstrates that the polymer chain dynamics are affected at distances greater than the characteristic size of the unperturbed chain. Earlier interpretations of experiments of the thermal expansion of ultrathin polymer films[5,35] have focused on either the substrate surface or the free surface. Here, we show that the substrate−polymer interaction can affect the dynamics at the free surface of thin polymer films.

When the film thickness is greater than 3 R_g, there are small differences between the thickest film examined here, sample E, and the results from Kunz and Stamm.[19] The chain distortion at the polymer−polymer interface for this sample and larger samples should not differ and the middle of the deuterated layer has bulk polymer-like conformations. As a result, the short time interdiffusion studied here does not probe length scales that reach significantly into polymer chains that are perturbed by the substrate either directly or indirectly through the adsorbed chain structure. Longer length scale experimental techniques will need to account for the surface effects on the dynamics since the adsorbed layer structure as well as the segment−segment exchange rate will become important.

Interesting questions remain regarding the effects of the polymer−substrate interaction energy and the molecular weight of the polymer. Currently, it is not clear how polymer chain dynamics from different sized polymer films are affected over a range of polymer−substrate interaction energies. For neutral surfaces, computer simulations suggest that the center of mass diffusion rate perpendicular to a wall is still reduced, but the lateral diffusion rate is enhanced.[11,14] These effects were observed only for distances less than R_g and for polymers well below the entanglement molecular weight. The SIMS experiment of Zheng et al.[9] for very thin polystyrene layers on silicon showed no difference in the effective diffusion constant from silicon oxide or hydrogen passivated silicon surfaces even though the polymer−substrate interaction energies are quite different. The very thin polymer layers used may involve enough contacts per chain to reduce the impact of the differences in the interaction energy at elevated temperatures. Further experiments measuring the initial stages of interdiffusion with systems with different polymer−substrate interaction energies or different temperatures are underway and should provide insight into their effect on interfacial polymer dynamics. Additionally, the molecular weight dependence of the interdiffusion dynamics will provide information about the extent of the adsorbed layer structure.

5. Summary and Conclusion

Neutron reflectometry is used to study the interdiffusion of PMMA bilayers with the polymer−polymer interface located near an attractive substrate. The concentration profile of the labeled (deuterated) layer is measured as a function of annealing time above the glass transition temperature of the polymer. The experimental technique provides detailed information about the initial interdiffusion ($\Delta\sigma < R_g$). The effect of the initial film thickness on the interdiffusion rate is studied to gain insight into the effect of chain confinement and polymer−substrate interaction energies on the chain dynamics as well as to provide an estimate of the length scale at which the substrate no longer perturbs the polymer dynamics.

The rate of interdiffusion is found to be strongly dependent upon the lower film size. Bulk interdiffusion behavior appears to be recovered for films 3−4 R_g thick. Different effective diffusion constants and time scaling behavior of the interfacial widths are observed and correlated with the polymer chain conformations and the polymer−substrate interaction energy. For films less than R_g thick, the effective diffusion constant is 2 orders of magnitude less than that of the thickest films. The significantly reduced mobility is attributed to the chain conformations being distorted parallel to the substrate and the numerous contacts per chain with the attractive surface. For films between 1 and 2 R_g thick, the effective diffusion constant is also less than that of the thickest layers, but greater than that of the thinnest layers. The reduced mobility from these layers is slightly due to direct chain contact with the substrate, but is primarily related to entanglements of the polymer chains near the polymer−polymer interface with the adsorbed structure of the chains closest to the substrate. These measurements directly show how polymer chain connectivity can effect changes on the polymer dynamics more than R_g from the surface.

Acknowledgment. We gratefully thank R. Wool and K. Welp for the use of their oven used in the annealing of some samples. E.K.L. acknowledges the support of the NIST-NRC Postdoctoral Research Associate Program.

References and Notes

(1) Sanchez, I. C. *Physics of Polymer Surfaces and Interfaces*; Butterworth-Heinemann, Boston, MA, 1992.
(2) Orts, W. J.; van Zanten, J. H.; Wu, W. L.; Satija, S. K. *Phys. Rev. Lett.* **1993**, *71*, 867.
(3) Keddie, J. L.; Jones, R. A. L.; Cory, R. A. *Europhys. Lett.* **1994**, *27*, 59.
(4) Reiter, G. *Macromolecules* **1994**, *27*, 3046.
(5) Wallace, W. E.; van Zanten, J. H.; Wu, W. L. *Phys. Rev. E.* **1996**, *52*, R3329.
(6) Wu, W. L.; van Zanten, J. H.; Orts, W. J. *Macromolecules* **1995**, *28*, 771.
(7) van Zanten, J. H.; Wallace, W. E.; Wu, W. L. *Phys. Rev. E* **1996**, *53*, R2053.
(8) Forrest, J. A.; Dalnoki-Veress, K.; Stevens, J. R.; Dutcher, J. R. *Phys. Rev. Lett.* **1996**, *77*, 2002.

(9) Zheng, Z.; Sauer, B. B.; van Alsten, J. G.; Schwartz, S. A.; Rafailovich, M. H.; Sokolov, J.; Rubinstein, M. *Phys. Rev. Lett.* **1995**, *74*, 407.
(10) van Alsten, J. G.; Sauer, B. B.; Walsh, D. J. *Macromolecules* **1992**, *25*, 4046.
(11) Mansfield, K. F.; Theodorou, D. N. *Macromolecules* **1989**, *22*, 3143.
(12) Bitsanis, I.; Hadziioannou, G. *J. Chem. Phys.* **1990**, *92*, 3827.
(13) Winkler, R. G.; Matsuda, T.; Yoon, D. Y. *J. Chem. Phys.* **1993**, *98*, 729.
(14) Baschnagel, J.; Binder, K. *J. Phys. 1 (Fr.)* **1996**, *6*, 1271.
(15) Baschnagel, J.; Binder, K. *Macromolecules* **1995**, *28*, 6808.
(16) Stamm, M.; Huttenbach, S.; Reiter, G.; Springer, T. *Europhys. Lett.* **1991**, *14*, 451.
(17) Karim, A.; Mansour, A.; Felcher, G. P.; Russell, T. P. *Phys. Rev. B* **1990**, *42*, 6846.
(18) Karim, A.; Felcher, G. P.; Russell, T. P. *Macromolecules* **1994**, *27*, 6973.
(19) Kunz, K.; Stamm, M. *Macromolecules* **1996**, *29*, 2548.
(20) de Gennes, P. G. *Scaling Concepts in Polymer Physics*; Cornell University Press: Ithaca, NY, 1979.
(21) Doi, M.; Edwards, S. F. *The Theory of Polymer Dynamics*; Oxford University Press: Oxford, England, 1986.
(22) Agrawal, G.; Wool, R. P.; Dozier, W. D.; Felcher, G. P.; Zhou, J.; Pispas, S.; Mays, J. W. *J. Polym. Sci., B: Polym. Phys.* **1996**, *34*, 2919.
(23) According to ISO 31−8, the term "molecular weight" has been replaced by "relative molecular mass," symbol M_r. Thus, if this nomenclature and notation were to be followed in this publication, one would write $M_{r,n}$ instead of the historically conventional M_n for the number average molecular weight, with similar changes for M_w, M_z, and M_v, and it would be called the "number average relative molecular mass". The conventional notation, rather than the ISO notation, has been employed for this publication.
(24) Certain commercial equipment and materials are identified in this paper in order to specify adequately the experimental procedure. In no case does such identification imply recommendation by the National Institute of Standards and Technology nor does it imply that the material or equipment identified is necessarily the best available for this purpose.
(25) The data throughout this manuscript, in the figures, and in the tables are presented along with the standard uncertainty (±) involved in the measurement.
(26) Williams, M. L.; Landel, R. F.; Ferry, J. D. *J. Am. Chem. Soc.* **1955**, *77*, 3701.
(27) Ankner, J. F.; Majkrzak, C. J. In *Neutron Optical Devices and Applications*; SPIE Proceedings 1738; SPIE: Bellingham, WA, 1992; p 260.
(28) Zhang, H.; Wool, R. P. *Macromolecules* **1989**, *22*, 3018.
(29) Clarke, C. J. *Polymer* **1996**, *37*, 4747.
(30) O'Connor, K.; McLeish, T. *Faraday Discuss. Chem. Soc.* **1994**, *98*, 67.
(31) Hariharan, A.; Kumar, S. K.; Russell, T. P. *J. Chem. Phys.* **1993**, *99*, 656.
(32) Liu, Y.; Reiter, G.; Kunz, K.; Stamm, M. *Macromolecules* **1993**, *26*, 2134.
(33) Frank, B.; Gast, A. P.; Russell, T. P.; Brown, H. R.; Hawker, C. *Macromolecules* **1996**, *29*, 6531.
(34) Douglas, J. F.; Johnson, H. E.; Granick, S. *Science* **1993**, *262*, 2010.
(35) Keddie, J. L.; Jones, R. A. L.; Cory, R. A. *Faraday Discuss. Chem. Soc.* **1994**, *98*, 219.
(36) Brandrup, J.; Immergut, E. H. *Polymer Handbook: Third Edition*, John Wiley & Sons: New York, 1989.

MA9704424